#### **SNAME Maritime Convention 2024**

14-16 October 2024, Norfolk, VA Copyright © 2024 Society of Naval Architects and Marine Engineers (SNAME) www.sname.org



# **Analyzing Tension Force and Fatigue Damage of WECs Mooring System**

# Wei-Ying Wong<sup>1</sup> (SM), Jia Mi<sup>1,2</sup> (V), Ta-Chih Hung<sup>1</sup> (SM), Lei Zuo<sup>1</sup> (V)

- 1. Department of Naval Architecture and Marine Engineering, University of Michigan, Ann Arbor, MI, USA
- 2. Department of Civil, Environmental and Ocean Engineering, Stevens Institute of Technology, Hoboken, 07030, USA

This study presents an analysis of the fatigue damage experienced by mooring systems under extreme and operational wave conditions, with a discussion on the Reference Model 3 (RM3), a widely recognized point absorber wave energy converter (WEC), and the Reference Model 5 (RM5), a floating oscillating surge wave energy converter (FOSWEC). Utilizing the combined capabilities of WEC-Sim and MoorDyn, both open-source simulation tools, the study investigates the dynamic behavior of mooring lines over the operational wave condition and a 100-year return period extreme wave condition. This study highlights the relationship between tension force and fatigue damage in mooring lines. The tension forces at various nodes of the mooring lines are calculated, revealing that the complex mooring design is causing a complex trend on the fatigue damage. Instead, variations in tension force show a more significant impact on cumulative fatigue damage, as evidenced by the higher damage observed in nodes experiencing greater tension variation. The findings contribute to a better understanding of the factors influencing fatigue damage in mooring lines of WECs and fatigue damage of different types of WECs, offering insights for more effective monitoring and strategies for WEC design optimization.

KEY WORDS: Mooring	system; wave	energy	converter;
tension force time history; cun	nulative fatigue	damage;	MoorDyn.

#### **NOMENCLATURE**

A	Cross-sectional area of mooring chain					
AEP	Annual energy production					
D	Cumulative fatigue damage					
DNVGL	Det Norske Veritas (Norway) and Germanischer Lloyd (Germany)					
<b>GWEC</b>	Global Wind Energy Council					
$H_{\rm s}$	Significant wave height					
i	Specific stress range in cumulative damage calculation					
JPD	Joint probability distribution					
k	Total number of stress ranges					
LCOE	Levelized cost of energy					
ML	Mooring line					
n	Number of cycles counted					
N	Number of cycles in the estimated stress where failure occurs					

PCC Power conversion chain

PTO Power take-off

RM3 Reference Model 3

RM5 Reference Model 5 S Stress range T Tension force  $T_p$  Peak wave period

WEC Wave energy converter

#### INTRODUCTION

Mooring line failures present significance challenges in the offshore structures including Oil and Gas (O&G) production platforms and offshore renewable energy platforms. Ma et al. (Ma et al. 2013) mentioned occurrences of early-life failures in mooring systems, the causes of which remain elusive. Fatigue analysis is a critical component in the design of offshore structure (DNVGL-RP-C203, 2019), and extensive research has been conducted on the fatigue analysis of mooring systems for O&G production platforms (Wu et al. 2015; Wu, Wang, and Eide 2015; Xue et al. 2018). In recent decades, the advancement of floating offshore wind platforms has increased by leveraging the experience of O&G industry. As reported in the Global Offshore

Analyzing Tension Force and Fatigue Damage of WECs Mooring System

SMC 2024, 14-16 October 2024, Norfolk, VA

Wind Report 2023 (GWEC, 2023), by the end of 2022, the global installation of net floating wind capacity reached 187.8 MW. Consequently, the mooring systems of floating wind platforms have been the focus of numerous recent studies (Sørum et al. 2023; Gao et al. 2021; Barrera et al. 2020). In addition to offshore floating structures that are already commercially operational which produced carbon-based fuel and offshore wind energy, ocean waves also offer as a promising resource of offshore renewable energy. As reported by M. Lehmann et al. (Lehmann et al. 2017), the maximum potential resource of wave energy in the United States along 100-m-depth ocean region is 522 TWh/yr. The study also mentioned that considering the wave energy converters (WECs) technology can extract 5% of the resource, the ocean waves could provide power up to 6-8 million (5%-7%) U.S. homes. The high cost and Levelized Cost of Energy (LCOE) of floating wind turbines have resulted in the increase attention on the development of wave energy harvesting technology. As an alternative energy harvester in the deep ocean, WECs present a promising opportunity to develop low-cost solutions during the R&D stage.

Given the increasing demand of offshore renewable energy to achieve the carbon net-zero goal by 2050, it is crucial to investigate the performance of mooring systems that provide station keeping for the WEC device during operational stage and extreme conditions. Therefore, the design and fatigue analysis of mooring systems for different types of WEC are of paramount importance. One benefit of designing mooring systems for WECs is the opportunity to leverage practical experience and lessons learned from commercial projects from offshore O&G and wind power sectors to mitigate risks during the design phase of future endeavors. However, most of the WEC developers focused more on the development of the geometry and power performance of the WEC devices and most of the time efforts on the design of the mooring systems is minimal. Ambühl et al. (Ambühl et al. 2015) investigated the fatigue reliability of Wavestar prototype structure, a bottom-fixed point absorber WEC. Yang et al. (Yang et al. 2016) shed the light on the fatigue damage result in a time duration of one minute along the mooring lines of a commercial floating point absorber WEC developed by a company Waves4Power ("Waves4Power," 2016). Even though Xu et al. (Xu et al. 2019) gave a review of mooring design and fatigue assessment of floating WEC, most of the fatigue assessment studies reported by them were focused on the floating structures in offshore O&G and wind power sectors, very few studies focused on the fatigue assessment of WEC's mooring system. Nonetheless, the trend does not imply that the fatigue damage analysis is unimportant for floating WEC, as a floating WEC structure has more cyclic motion compared with floating platform of O&G and wind sectors due to its interaction with waves. In this regard, this study aims to examine the tension load and fatigue damage of the Reference Model 3 (RM3) (Neary et al., 2014) and Reference Model 5 (RM5) (Yu et al. 2015) WECs' mooring system.

RM3 is a two-body floating wave point absorber which harvest the wave energy from the heave motion of a surface float, while RM5 is a floating oscillating surge WEC which harvest

Analyzing Tension Force and Fatigue Damage of WECs Mooring
System

Lei Zuo

energy through the surge motion of a flap body. These reference models, which were developed by national laboratories and published in recent years, are intended to function as open-source study objects. The purpose of developing reference models for WECs is to facilitate in-depth research and generate insights by the WEC R&D community regarding these benchmarked floating WEC designs. As most of the studies focused more on investigating the improvement of the hydrodynamics and power take-offs (PTOs) of the RMs, very few studies investigate the performance of the mooring systems. This arises a question that which type of WEC provides less influence of cyclic load motion to the mooring system as it is crucial having a robust stationkeeping system during the extreme conditions. Despite of analyzing the tension results of the mooring lines, the cumulative fatigue damage is an important index as well. The cumulative fatigue damage is evaluated using the rain-flow counting method and Palmgren-Miner rule which the guidelines can be found from governing rules and standards (DNVGL-RP-C203, 2019; ASTM, 2017; DNV-OS-E301, 2021). The stress range and number of cycles are determined from the S-N curve as defined in the standard (DNV-OS-E301, 2021), while the stress history of the mooring line under different wave conditions can be derived from numerical simulation tool such as MoorDyn. The main objective of this study is therefore to compare the tension results and fatigue damage of the mooring system of the RM3 and RM5.

The structure of this paper is organized as follow: Section 2 includes the introduction of the RM3 and RM5 wave energy converters and its mooring system, and the procedure of the mooring tension analysis and fatigue damage assessment. The Section 3 presents the results of the tension variation results in time domain on selected nodes, and the fatigue damage results along the mooring line. The conclusions of this study are provided in the last section.

## **METHODOLOGY**

In this study, we consider the RM3 (Neary et al., 2014) and RM5 designed by national labs (Yu et al., 2015). For numerical simulation purposes, we employ the open-source software WEC-Sim (Ogden et al. 2022), which is capable of simulating the hydrodynamic bodies, joints, constraints, PTO systems, and mooring systems of WECs. We utilize MoorDyn (Hall and Goupee, 2015), a lumped-mass based model, to model the dynamics of the mooring lines by coupling with WEC-Sim. The tension at each node of the mooring line is simulated using this combined setup and subsequently apply these tension results to estimate the fatigue damage.

#### **Site Conditions**

According to Neary et al. (Neary et al., 2014) and Yu et al. (Yu et al. 2015), both RM3 and RM5 WEC were developed for a reference site situated offshore near Eureka in Humboldt County, California. Fig. 1 illustrates the reference site has a characteristic of mild sloping seafloor, resulting in a relatively uniform wave field. The water depth varies between 40 and 100 meters. Additionally, Table 1 presents the wave scatter diagram for the

reference site, which depicts the joint probability distribution (JPD) of significant wave height and wave period occurrences over a year. The two WECs design considered the 100-year return period extreme sea state as the device's survivability design criteria. The 100-year return period of significant wave height and peak wave period was evaluated using 20-year of measured data from 10 buoys positioned in proximity to the reference site (Neary et al., 2014; Berg 2011).

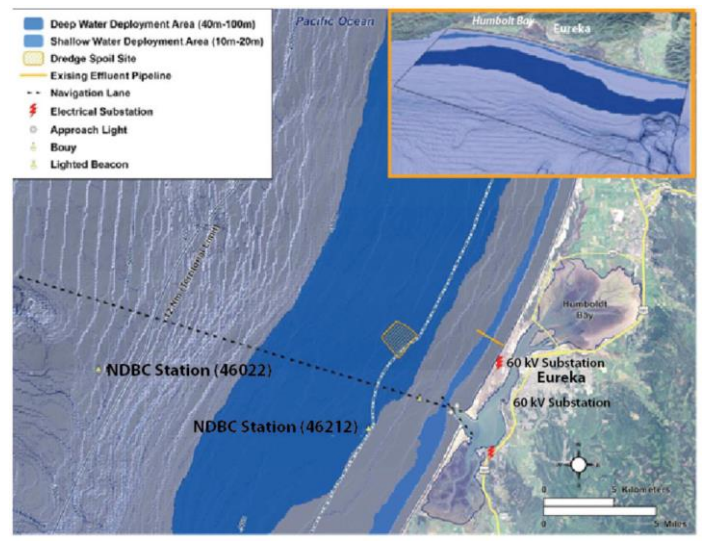


Fig. 1, Reference site bathymetry plan (Neary et al., 2014)

Table 1. Percentage of Total Energy of Sea States at Humboldt Bay, California (Neary et al., 2014)

							Join	t Prob	ability I	Plot (%)	)						
										Ге							
_		4.5	5.5	6.5	7.5	8.5	9.5	10.5	11.5	12.5	13.5	14.5	15.5	16.5	17.5	18.5	19.5
	0.25	0.0%	0.0%	0.0%	0.0%	0.0%	0.0%	0.0%	0.0%	0.0%	0.0%	0.0%	0.0%	0.0%	0.0%	0.0%	0.0
	0.75	0.0%	0.0%	0.6%	0.8%	0.5%	0.5%	0.2%	0.0%	0.0%	0.0%	0.0%	0.0%	0.0%	0.0%	0.0%	0.0
	1.25	0.0%	1.0%	2.7%	3.7%	4.1%	2.9%	1.5%	0.4%	0.1%	0.0%	0.0%	0.0%	0.0%	0.0%	0.0%	0.0
	1.75	0.0%	1.0%	4.4%	4.3%	4.1%	3.4%	2.0%	1.1%	0.6%	0.1%	0.0%	0.0%	0.0%	0.0%	0.0%	0.0
	2.25	0.0%	0.2%	3.5%	4.2%	3.6%	4.1%	3.1%	1.5%	1.2%	0.3%	0.0%	0.0%	0.0%	0.0%	0.0%	0.0
	2.75	0.0%	0.0%	1.5%	2.5%	1.9%	3.2%	3.3%	1.8%	1.1%	0.4%	0.1%	0.1%	0.0%	0.0%	0.0%	0.0
	3.25	0.0%	0.0%	0.1%	0.9%	0.9%	2.0%	2.4%	1.4%	0.8%	0.4%	0.1%	0.0%	0.0%	0.0%	0.0%	0.0
	3.75	0.0%	0.0%	0.0%	0.1%	0.2%	1.0%	1.9%	1.5%	0.5%	0.3%	0.2%	0.1%	0.0%	0.0%	0.0%	0.0
	4.25	0.0%	0.0%	0.0%	0.0%	0.0%	0.2%	1.0%	1.3%	0.5%	0.3%	0.2%	0.1%	0.0%	0.0%	0.0%	0.0
[	4.75	0.0%	0.0%	0.0%	0.0%	0.0%	0.0%		400	10000000		100000000000000000000000000000000000000		100000000000000000000000000000000000000	0.0%	0.0%	0.0
Is	5.25	0.0%	0.0%	0.0%	0.0%	0.0%	0.0%	0.1%	0.2%	0.3%	0.2%	0.1%	0.0%	0.0%	0.0%	0.0%	0.0
	5.75	0.0%	0.0%	0.0%	0.0%	0.0%	0.0%			0.1%				100000000000000000000000000000000000000	0.0%	0.0%	0.0
	6.25	0.0%	0.0%	0.0%	0.0%	0.0%	0.0%	0.0%	0.1%	0.1%		0.0%	0.0%	0.0%	0.0%	0.0%	0.0
	6.75	0.0%	0.0%	0.0%	0.0%	0.0%	0.0%	0.0%	0.0%	0.0%	100000000000000000000000000000000000000	100000000	2000		0.0%	0.0%	0.0
	7.25	0.0%	0.0%	0.0%	0.0%	0.0%	0.0%		and the same						0.0%	0.0%	
ı	7.75	0.0%	0.0%	0.0%	0.0%	0.0%	0.0%			0.0%			0.0%		0.0%	0.0%	0.0
ı	8.25	0.0%	0.0%	0.0%	0.0%	0.0%	0.0%		0.0%	0.0%	100000000000000000000000000000000000000	0.0%	0.0%		0.0%	0.0%	0.0
ı	8.75	0.0%	0.0%	0.0%	0.0%	0.0%	0.0%		0.0%	0.0%		0.0%	0.0%		0.0%	0.0%	0.0
ı	9.25	0.0%	0.0%	0.0%	0.0%	0.0%	0.0%						0.0%				
_	9.75	0.0%	0.0%	0.0%	0.0%	0.0%	0.0%		0.0%	0.0%	0.0%		0.0%	0.0%	0.0%		

#### **RM3 and RM5 Wave Energy Converters**

Based on the site conditions and the design methodology mentioned by Neary et al. (Neary et al., 2014), the general design and dimensions of the RM3 WEC device is illustrated in Fig. 2. The RM3 device has a total weight of 680 Tonnes. This device consists of a surface float that translates the wave motion relative to the vertical column spar buoy. The surface float is designed to be able to oscillate along the vertical column up to 4 meters. The device is intended for deployment in water depths ranging from

40 to 100 meters. Additionally, the RM3 design incorporates a hydraulic power conversion chain (PCC) system housed within the vertical column. Optimal energy capture by a wave point absorber is achieved at resonance, meaning the velocity of the oscillating body is synchronized with the hydrodynamic wave excitation force. The rated power and the annual energy production (AEP) of the RM3 is 286 kW and 700 MWh, respectively, as reported by Neary et al.

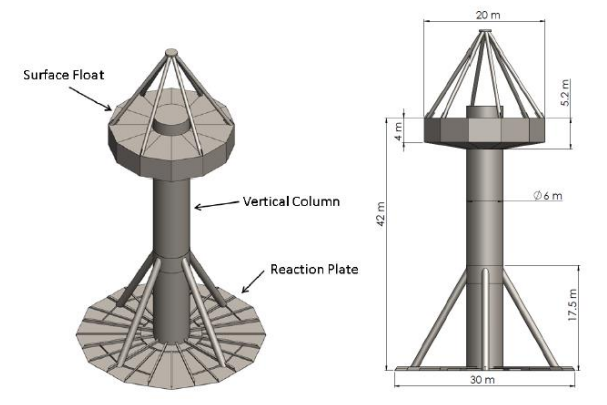


Fig. 2, RM3 device design and dimensions (Neary et al., 2014)

As reported by Yu et al. (Yu et al., 2015), the RM5 design incorporates a flap and a supporting frame constructed from steel tubes, and four tension legs as the mooring system. The general design and dimensions of the RM5 WEC are illustrated in Fig. 3. The total weight of this device is 800 Tonnes. The RM5 captures energy through the motion of the flap, which rotates against the supporting frame in response to the surge motion of incoming waves. The RM5 is specifically designed for deployment in deepwater environments (50 m - 100 m), necessitating a mooring system to maintain its position. The RM5's rated power output is 360 kW, and its annual energy production (AEP) is reported at 882 MWh. The RM5 exhibits a higher rated power output and greater weight compared to the RM3. However, when considering the order of magnitude, both WECs possess comparable levels of rated power and weight. Therefore, these two wave energy reference models assure a comparative analysis.

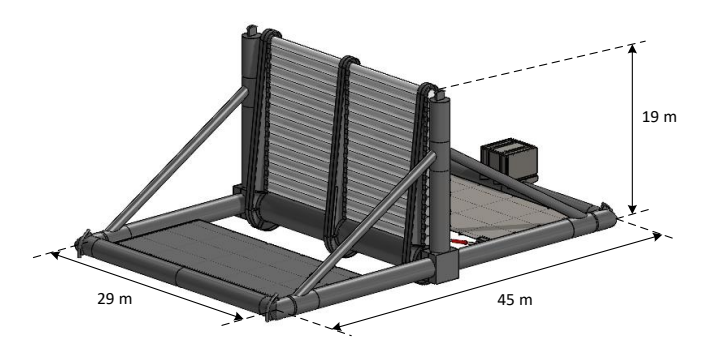


Fig. 3, RM5 device design and dimensions (Yu et al., 2015)

#### **Mooring Design and Analysis**

The design of the mooring system for the RM3 and RM5 WECs is intended to survive in extreme sea conditions. Table 2 outlines the essential requirements for the mooring system. As reported by Neary et al. (Neary et al., 2014), for a sea state with a 100-year return period, the extreme mooring load is estimated to be 1886 kN. To ensure safety, a required breaking strength of 3680 kN is determined by applying a safety factor of 1.95. The configuration of the mooring system is designed to accommodate these specifications.

Table 2. Mooring design requirements [Reproduced from (Neary et al., 2014)]

Water Depth	70 m
100-year Significant Wave Height ( <i>H</i> <sub>s</sub> )	11.9 m
100-year Peak Wave Period (T <sub>p</sub> )	17.1 s
100-year Current Speed	0.59 m/s
Seafloor Composition	Sand/ Clay
Mooring legs	Chain $(d = 89 \text{ mm})$
Anchors	Drag Embedment

As depicted in Fig. 4, the mooring system of the RM3 comprises three mooring legs, each exhibiting a catenary profile. To mitigate the vertical force components exerted on the mooring line, a subsea buoy with a net uplift capacity of 55 kN is integrated into each mooring leg. The mooring lines are positioned 120 degrees apart, with the first mooring line placed parallel to the direction of incoming waves.

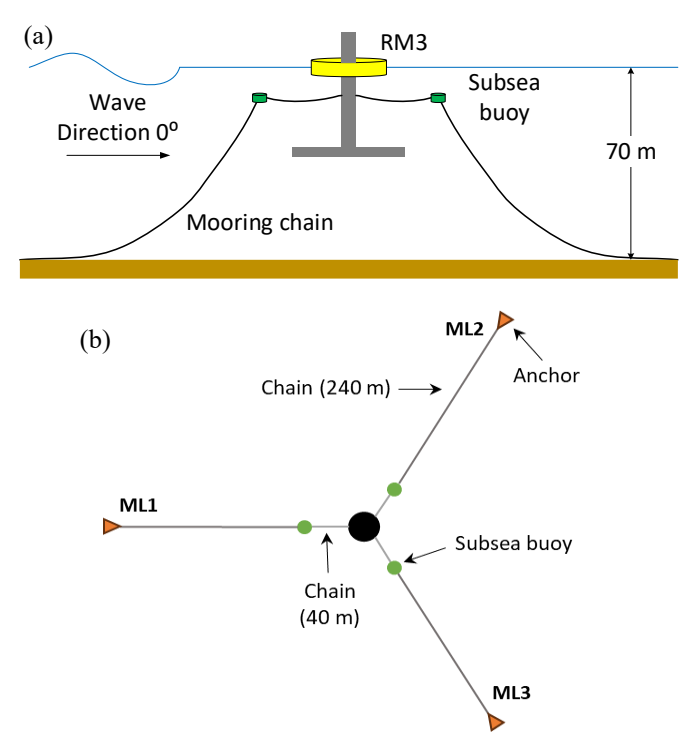


Fig. 4, Mooring system configuration and dimensions of RM3 (not in scale).

Analyzing Tension Force and Fatigue Damage of WECs Mooring System Lei Zuo

Fig. 5 illustrates the mooring system design of the RM5, which features four mooring legs, each characterized by a catenary profile. The decision to change the mooring lines of RM5 from a tension leg system (Yu et al., 2015) to a catenary profile is based on two primary reasons. First, the installation cost of the tension leg mooring system accounted for approximately 50% of the total installation cost due to the high pretension and anchoring load requirements. In contrast, catenary profile does not encounter these high requirements, significantly reducing installation costs. Secondly, using a similar mooring system for both devices ensures that the results are comparable, facilitating the investigation of the influence of different WEC devices on the same mooring system. Unlike the RM3, the RM5's mooring lines are not equipped with subsea buoys. The reason is the uplift force provided by the subsea buoys will increase the heave response, which could diminish the power generation performance of the flap as the draft increase. The mooring lines are positioned 90 degrees apart, with the initial mooring line set at a 45-degree angle relative to the direction of incoming waves.

The tension force along the mooring line is simulated through the integration of two open-source simulation tools, WEC-Sim and MoorDyn, both of which have been well validated for simulating WEC and mooring line dynamics. Table 3 shows the properties and hydrodynamic coefficients of mooring line considered in the MoorDyn simulation.

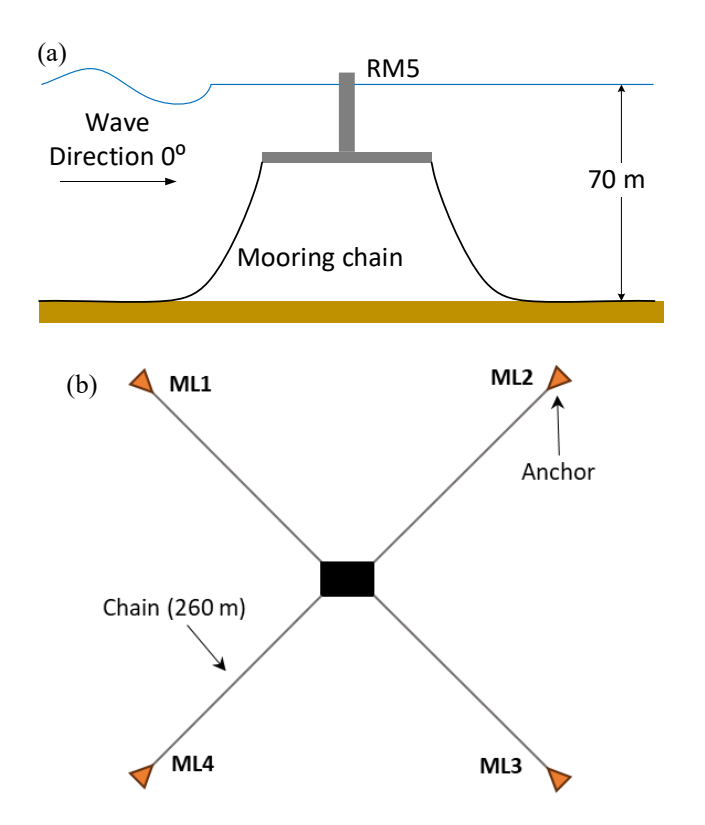


Fig. 5, Mooring system configuration and dimensions of RM5 (not in scale).

To examine the effects of wave excitation, an irregular wave profile using the JONSWAP wave spectrum from the 0° direction is modeled. Table 4 lists the wave conditions considered in the simulation. The first bin represents the 100-yr return period wave condition, while the second bin describes an operational wave condition with a probability of occurrence of 4.1% as indicated by the wave scatter data (Table 1). The simulation, conducted using WEC-Sim and MoorDyn, spans a total of 3800 seconds with a time step of 0.01 seconds in WEC-Sim and 0.0005 seconds in MoorDyn. To avoid numerical instability at the beginning of the simulation, the initial and final 100 seconds of the simulated data are excluded from the fatigue damage assessment.

Table 3. Input data for RM3 and RM5 simulation in MoorDyn (WEC-Sim Documentation, 2023) (Neary et al., 2014)

wEC-Sili Documentation, 2023) (Neary et al., 2014)					
	RM3	RM5			
Number of Mooring Legs	3	4			
Line Type	Chain				
Volume-Equivalent Diameter	0.14	4 m			
Mass Density in Air	126.0 kg/m				
Axial Stiffness	xial Stiffness 583.376 x 10 <sup>6</sup>				
Normal Added Mass Coefficient	1.0				
Tangential Added Mass Coefficient	0.0				
Normal Drag Coefficient	1.6				
Tangential Drag Coefficient	0.05				

Table 4. Wave bins information

Bin	$H_{\rm s}$	$T_{ m p}$	Wave Condition
1	11.9 m	17.1 s	Extreme
2	2.25 m	9.5 s	Operational

#### **Fatigue Damage Assessment**

In this study, the fatigue damage is evaluated under both extreme and operational wave conditions. The fatigue damage assessment is conducted in time domain by following the governing rules and regulars (DNVGL-RP-C203, 2019; ASTM, 2017; DNV-OS-E301, 2021).

The fatigue analysis employs the rain-flow level-crossing counting method (ASTM, 2017), which identifies the number of cycles and stress amplitude from the time history of stress at the nodes of the mooring line. The time history of stress is derived from the tension force as simulated by MoorDyn.

To quantify the total damage, the S-N curve approach (DNV-OS-E301, 2021) is utilized together with the rain-flow counting method and the Palmgren-Miner rule (DNVGL-RP-C203, 2019). The relevant S-N curve for mooring analysis is represent by Equation (1):

Analyzing Tension Force and Fatigue Damage of WECs Mooring System Lei Zuo

$$S^m = \frac{a_D}{N_c} \tag{1}$$

where S represents stress range in MPa, defined as S = T/A, where A is the cross-sectional area in m<sup>2</sup>, and T is the tension force in kN. For studless chain, the parameters are  $a_D = 6 \times 10^{10}$  and m = 3.0.

The cumulative fatigue damage, D, is calculated according to the Palmgren-Miner rule which is expressed in the following equation:

$$D = \sum_{i=1}^{k} \frac{n_i}{N_i} \tag{2}$$

where i corresponds to a specific stress range, k is the total number of stress ranges, n is the number of cycles counted, and N is the number of cycles in the estimated stress where failure occurs as determined from the S-N curve.

#### **RESULTS AND DISCUSSION**

This section illustrates the results of the tension load of the nodes as simulated by MoorDyn and the evaluated fatigue damage along the mooring lines.

#### **Tension Force of Fairlead**

Two irregular wave bins in JONSWAP spectrum are modeled using WEC-Sim and MoorDyn over a duration of 3800 seconds. The tension force of each node of the mooring lines is derived from the outputs of MoorDyn. The aim of considering these two wave bins is to explore the fatigue damage induced by both extreme and operational wave conditions.

Fig. 6 and Fig. 7 demonstrate the wave elevation, the heave response of the platform, and fairlead tensions during time interval from 3000 s to 3600 s for the RM3 and the RM5, respectively, under the Bin 1 wave condition. For the RM5, as the configuration of mooring line (ML)1 and ML4, ML2 and ML3 are symmetric, therefore, for better visualization, the fairlead tension of ML1 and ML2 are shown. Notably, in both scenarios, the first mooring line—which is aligned parallel to the incident of the wave—exhibits a greater variation in tension force compared to the other two mooring lines. Additionally, the results reveal that the tension force fluctuates more significantly under extreme wave conditions than under operational wave conditions. While the RM3 has more drastic heave response under the same incoming waves condition with the RM5, it has higher tension force compared with the RM5. This implies that the absence of the subsea buoy in the mooring system of the RM5 provides a better result in terms of the tension force of the fairlead. These tension force readings are subsequently utilized to compute the stress time histories necessary for the fatigue damage assessment.

Fig. 8 and Fig. 9 display the wave elevation, the heave response of the platform, and the fairlead tensions for the RM3 and RM5, respectively, during the time interval from 3000 s to 3600 s under Bin 2 wave conditions. The fairlead tensions of both

WECs are lower than those observed under Bin 1 wave conditions. Additionally, the fairleads of the RM5 experience lower tension forces compared to those of the RM3, despite the similar heave responses exhibited by both WECs in this wave condition.

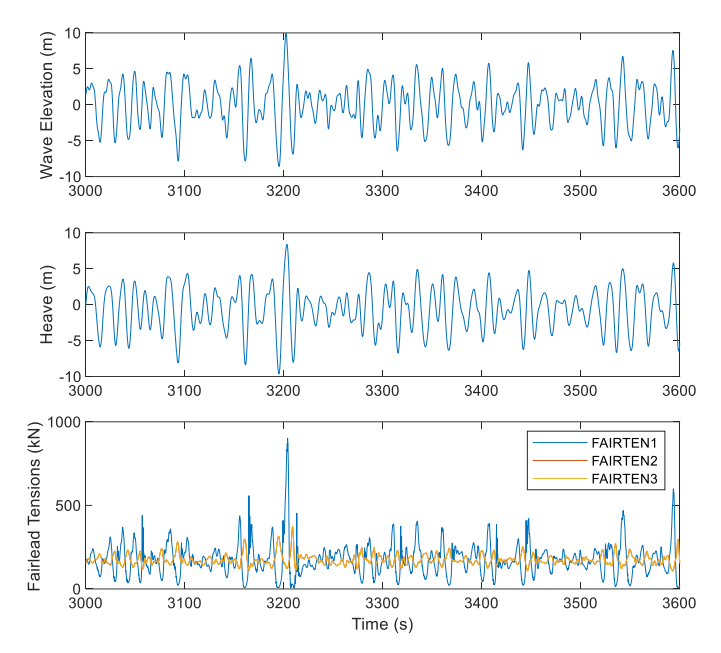


Fig. 6, Wave elevation, heave response, fairlead tensions under extreme wave condition for RM3.

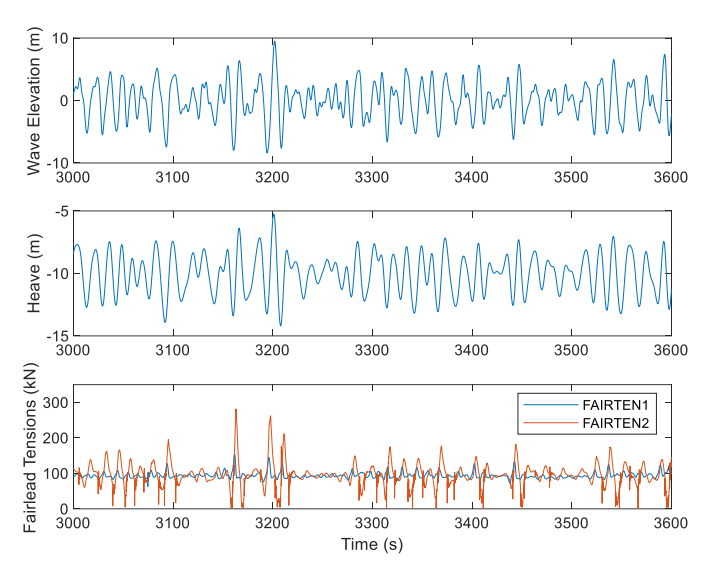


Fig. 7, Wave elevation, heave response, fairlead tensions under extreme wave condition for RM5.

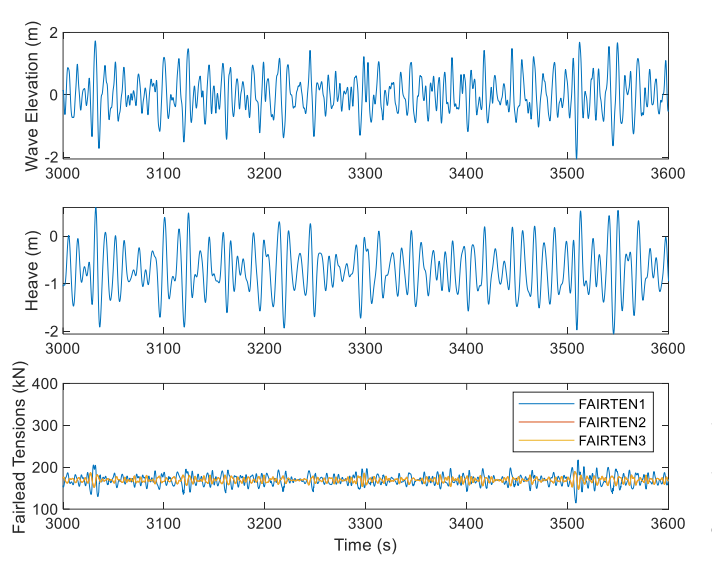


Fig. 8, Wave elevation, heave response, fairlead tensions under operational wave condition for RM3.

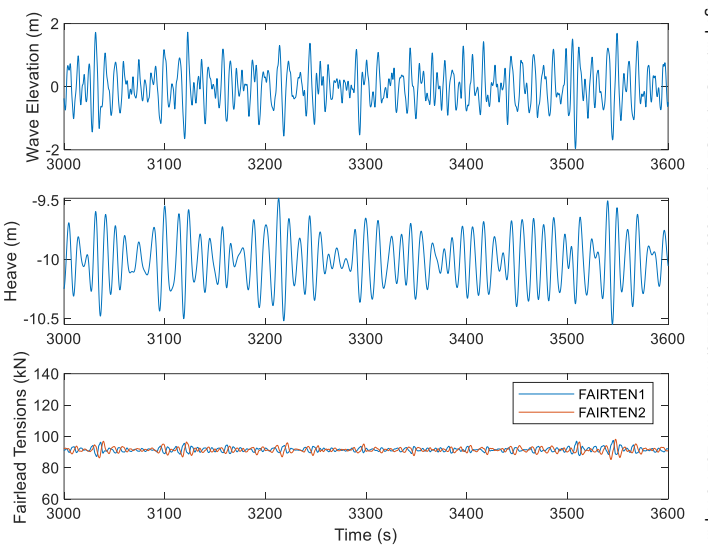


Fig. 9, Wave elevation, heave response, fairlead tensions under operational wave condition for RM5.

# **Tension Force and Fatigue Damage along Mooring Lines under Extreme Wave Condition**

Fig. 10 (a) illustrates the configuration of 1<sup>st</sup> mooring line (ML1) of the RM3. The tension forces of each node are calculated from MoorDyn, and the tension force of NODES 1, 3, 6, 8 under Bin 1 (extreme) wave condition are depicted in Fig. 10 (b). NODE 1 is the position of fairlead which connects with the platform. As shown in Fig. 10 (b), NODE 1 has the highest tension force, NODE 8 has the second highest tension force. NODE 3 has a larger tension force variation compared with NODE 6. As indicated in Fig. 10 (b), while NODE 1 bears the maximum tension force, it sustains the greatest fatigue damage, see Fig. 10 (c). Furthermore, in Fig. 10 (c), it is observed that NODE 3 incurs more fatigue damage than NODE 6, correlating with its larger tension force variation.

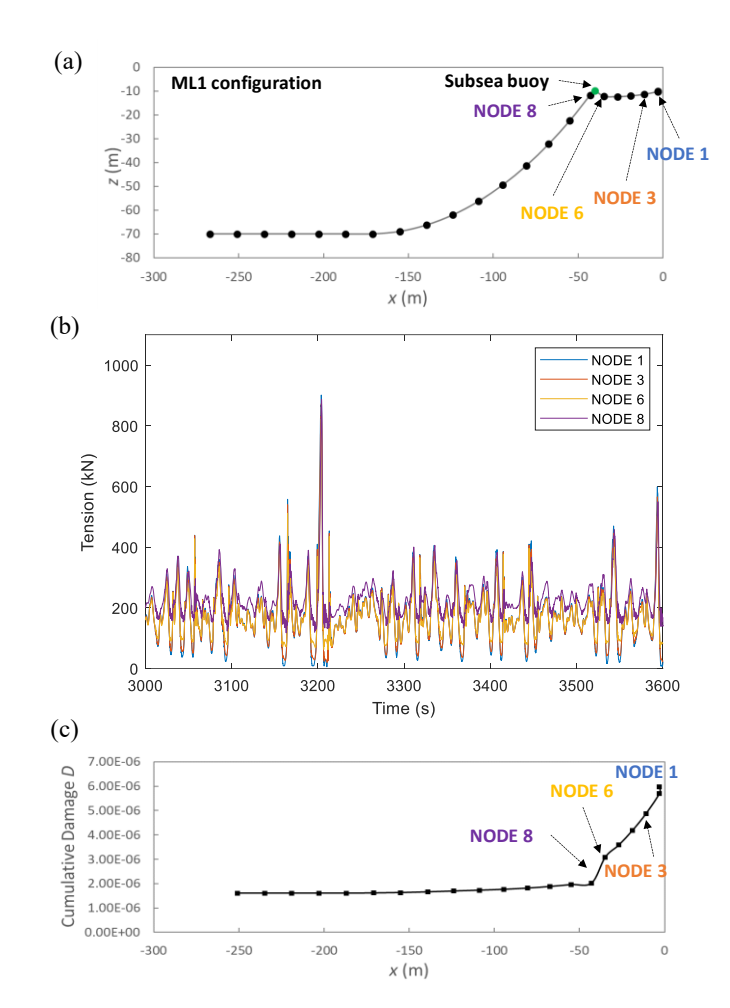
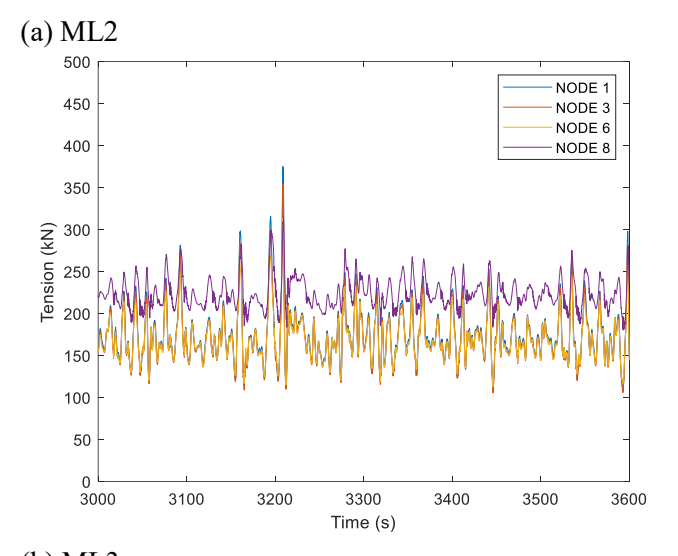


Fig. 10, Results of RM3: (a) Configuration of Mooring Line 1 (ML1); (b) Tension force of nodes on ML1 under extreme wave condition; (c) Cumulative fatigue damage along ML1 under extreme wave condition.

Fig. 11 presents a comparison of the mooring line tension of NODE 1 (Fairlead), NODE 3, NODE 6, and NODE 8 of 2<sup>nd</sup> mooring line (ML2) and 3<sup>rd</sup> mooring line (ML3), respectively. Given that ML2 is symmetrically deployed in relation to ML3, their tension force time histories are identical. Furthermore, to investigate the fatigue damage along ML2 and ML3, the same fatigue assessment is carried out for ML2 and ML3, the results are displayed in Fig. 12. Since the tension force time histories for both mooring lines are equivalent, their cumulative fatigue damages are also identical. Furthermore, the pattern of fatigue damage along ML2 and ML3 mirrors that observed in ML1, where the fairlead exhibits more damage than the other sections along the mooring line. Nonetheless, the overall fatigue damages for ML2 and ML3 are less than those for ML1, which is attributed to ML1 experiencing higher tension forces.

Analyzing Tension Force and Fatigue Damage of WECs Mooring System Lei Zuo



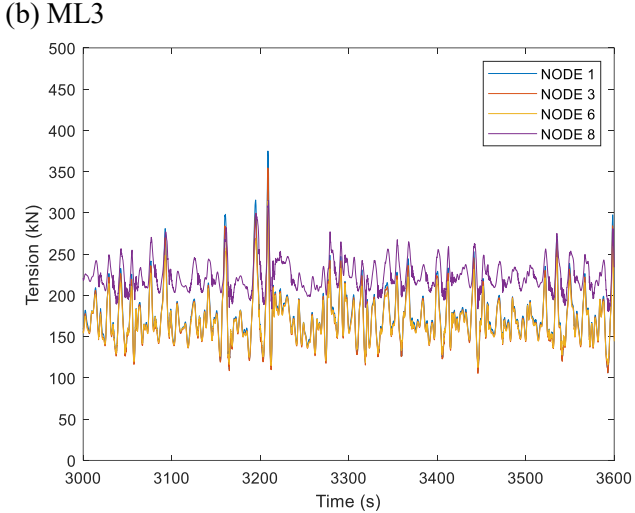


Fig. 11, Tension force of nodes on (a) ML2 and (b) ML3 under extreme wave condition, RM3. Since the configuration of ML2 and ML3 are symmetric, therefore both mooring lines have same results.

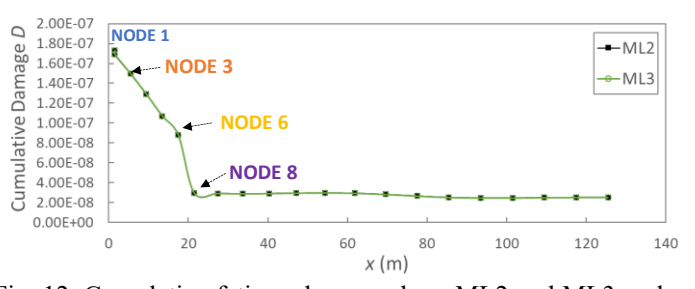


Fig. 12, Cumulative fatigue damage along ML2 and ML3 under extreme wave condition, RM3.

Regarding the mooring line profile of the RM5, Fig. 13 (a) illustrates the profile of ML1. Similar to the results shown for the RM3, the tension forces of each node are calculated from MoorDyn, and the tension force of NODES 1, 2, 3 under Bin 1

(extreme) wave condition are depicted in Fig. 13 (b). NODE 1 is the position of fairlead which connects with the platform. As indicated in Fig. 13 (b), NODE 1 has the highest tension force, following is the NODE 2 has the second highest tension force. As shown in Fig. 13(b), while Node 1 sustains the maximum tension force, it also incurs the greatest fatigue damage. A notable difference from the RM3 is that the fatigue damage of the mooring line near the anchor is higher than at the touchdown point of the mooring line (around x = -50 m), a phenomenon not observed under either wave condition in the RM3 case.

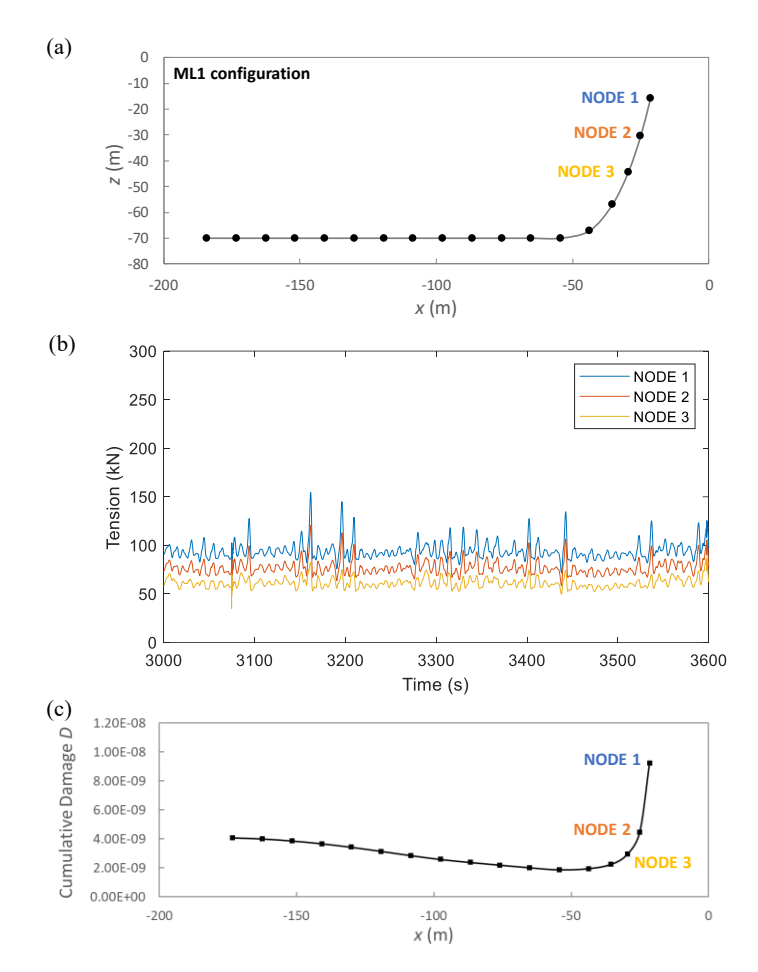


Fig. 13, Results of RM5: (a) Configuration of Mooring Line 1 (ML1); (b) Tension force of nodes on ML1 under extreme wave condition; (c) Cumulative fatigue damage along ML1 under extreme wave condition.

# **Tension Force and Fatigue Damage along Mooring Lines under Operational Condition**

To explore the tension force time history and associated fatigue damage along the mooring line under operational wave condition, the tensions at NODES 1, 3, 6, 8 under Bin 2 (operational) wave condition are shown in Fig. 14 (a) for the ML1 of RM3. Fig. 14 (a) reveals that NODE 1 no longer exhibits a higher tension force over the time compared to the other nodes in this wave condition, but slightly higher that other segments between the subsea buoy and the fairlead. However, unlike in Bin 1 wave condition, the cumulative fatigue damage at NODE 1 is slightly lower than other nodes as indicated in Fig. 14 (b). Furthermore, Fig. 14 (a) shows that while the average tension at NODES 3 and 6 is lower than at NODE 1 8, the variation of tension is greater. Consequently, NODES 3 and 6 experience more cumulative damage than NODE 8, suggesting a positive correlation between cumulative damage and the variation in tension force.

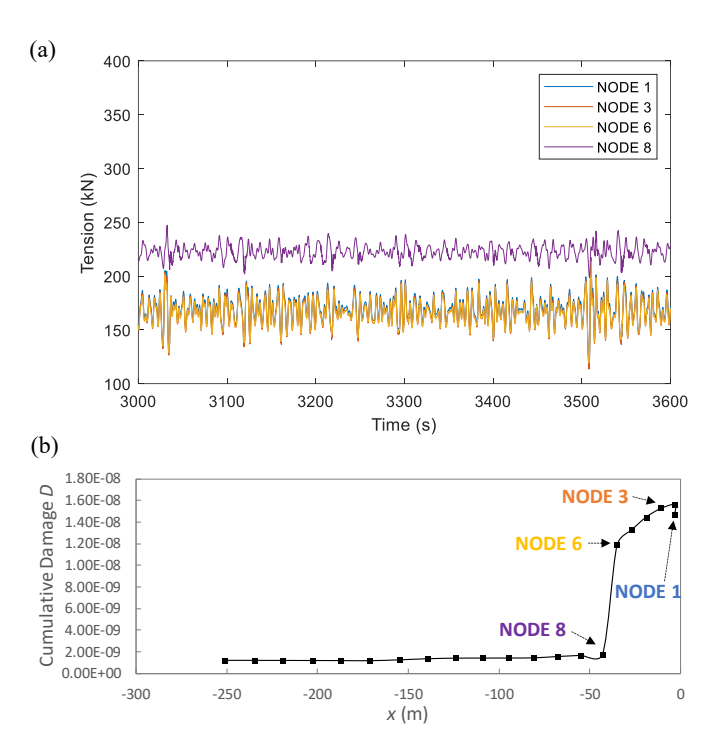
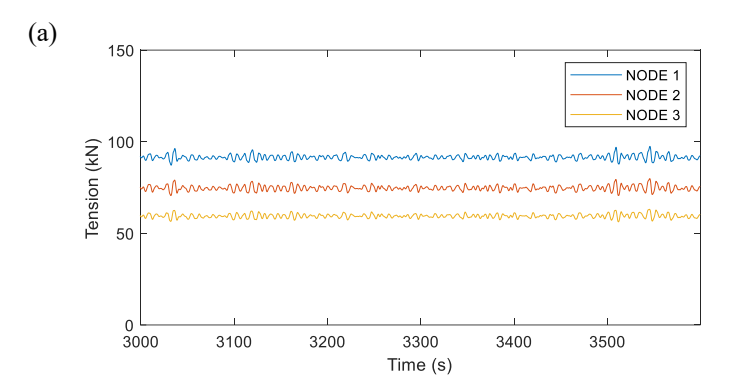


Fig. 14, Results of RM3: (a) Tension force of nodes on ML1 under operational wave condition; (b) Cumulative fatigue damage along ML1 under operational wave condition.

For the tension force time history and associated fatigue damage along the mooring line of the RM5 under operational wave condition, the tensions at NODES 1, 2, and 3 under Bin 2 wave condition are shown in Fig. 15 (a) for the ML1. Fig. 15 (a) reveals that NODE 1 remain exhibits a higher tension force over the time compared to the other nodes in this wave condition, same as the trend under extreme wave condition. The cumulative fatigue damage along ML1 also has a similar trend compared with extreme wave condition. These results imply that without the

existence of non-continuous point, such as the installation of a subsea buoy, will result in a more consistent of the fatigue damage under different wave conditions.



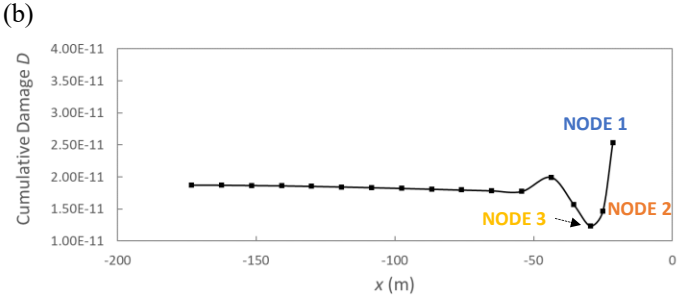


Fig. 15, Cumulative fatigue damage along ML1 under operational wave condition.

## Comparison of Tension and Fatigue Damage Results between RM3 and RM5

To provide a comprehensive view of the results, the highest tension forces of Mooring Line 1 (ML1) for both WECs under extreme and operational wave conditions have been extracted and compared in Fig. 16. It is demonstrated that the ML1 of the RM3 experiences a higher tension force compared to that of the RM5. Additionally, the highest cumulative fatigue damage of ML1 for both WECs under these conditions is also analyzed in Fig. 16. As previously mentioned, the RM5 exhibits lower cumulative fatigue damage relative to the RM3, attributed to a smaller amplitude of tension force fluctuation in the time domain. This comparison indicates that the RM5 has better performance than the RM3 in terms of both tension force and fatigue damage, displaying lower values in these indices.

#### **CONCLUSIONS**

This study has presented an analysis of cumulative fatigue damage along the mooring lines of the RM3 wave point absorber and RM5 oscillating surge wave energy converter under the influence of extreme and operational wave conditions. Utilizing the dynamic modeling capabilities of WEC-Sim coupled with the simulation of mooring line dynamics via MoorDyn, the authors have estimated the fatigue damage over a 100-year extreme wave event and an operational wave event, simulated over a time duration of an hour.

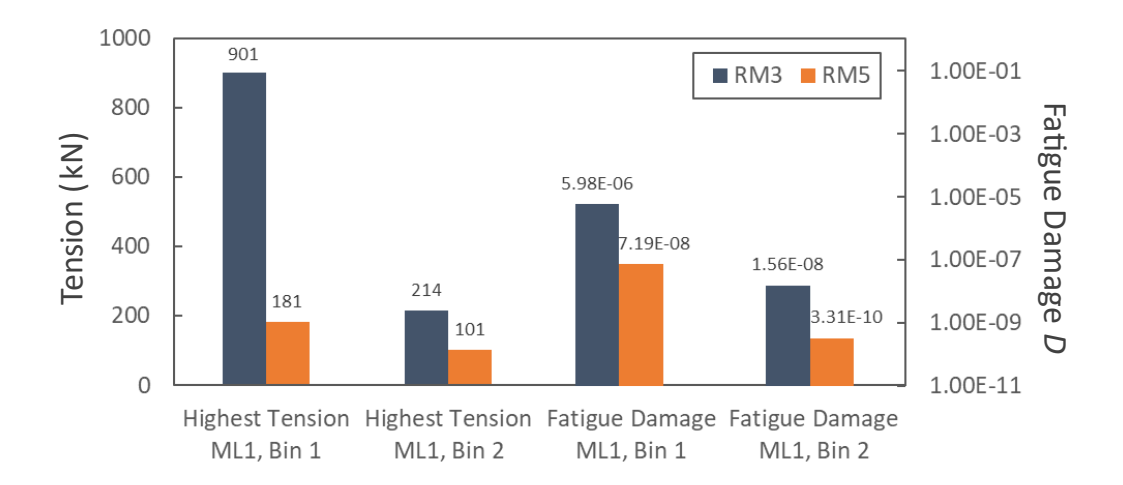


Fig. 16, Comparison of highest tension and fatigue damage of ML1 of RM3 and RM5 under Bin 1 (extreme) and Bin 2 (operational) wave conditions.

The findings of this study indicate that the trend of the cumulative fatigue damage for the mooring system of RM3 is different between extreme and operational wave conditions. This observation underscores the complex nature of fatigue phenomena where the local maxima of tension are not necessarily the predictors of the most significant damage. Instead, it is the variation in the tension force, rather than its peak values, that

exhibits a positive correlation with the cumulative fatigue damage. Furthermore, as the wave energy converters are designed to have the best performance during operational wave conditions, it is crucial to investigate the fatigue damage of the mooring lines under the operational wave condition of the desired site, instead of only investigate the maximum tension force of the mooring line under extreme wave condition. As mentioned

previously, for the floating structures of oil & gas drilling and production, there are numerous cases of mooring line failure in early stage without encountering the extreme wave condition (Ma et al. 2013) Therefore, this depicts the importance of looking at the fatigue damage of the mooring line.

In addition, the design of the mooring system will affect the power performance of the wave energy converters, as the mooring lines will produce restoring force that influences the motion response of the WEC under the wave excitations. Therefore, incorporating the mooring system design into the design optimization of WEC is essential.

Future research should focus on broadening the range of simulated conditions, including variable wave directions and multi-hour extreme scenarios, to enhance the understanding of fatigue damage distribution. Furthermore, considering the importance of multiple parameters in the design optimization process, the application of data-driven models, such as neural networks, could be explored in future studies.

#### ACKNOWLEDGEMENTS

The authors wish to thank partial funding support from DOE EERE (Grant #DE-EE0008390), NSF (Grant # 1738689), NOWRDC (project #131/192898), and the Seeding To Accelerate Research Themes (START) program of University of Michigan, Michigan Engineering.

#### **REFERENCES**

- Ambühl, Simon, Francesco Ferri, Jens Peter Kofoed, and John Dalsgaard Sørensen. 2015. "Fatigue Reliability and Calibration of Fatigue Design Factors of Wave Energy Converters." *International Journal of Marine Energy* 10 (June):17–38. https://doi.org/10.1016/j.ijome.2015.01.004.
- Barrera, Carlos, Tommaso Battistella, Raúl Guanche, and Iñigo J. Losada. 2020. "Mooring System Fatigue Analysis of a Floating Offshore Wind Turbine." *Ocean Engineering* 195 (January):106670. https://doi.org/10.1016/j.oceaneng.2019.106670.
- Berg, Jonathan. 2011. "Extreme Ocean Wave Conditions for Northern California Wave Energy Conversion Device." SAND2011--9304, 1113856, 457209. https://doi.org/10.2172/1113856.
- Position Mooring: DNV-OS-E301, 2021.
- E08 Committee. 2017. "Practices for Cycle Counting in Fatigue Analysis." ASTM International. Accessed December 11, 2023. https://doi.org/10.1520/E1049-85R17.
- Fatigue Design of Offshore Steel Structures: DNVGL-RP-C203. 2019. DNV GL AS.
- Gao, Xifeng, Xiaoyong Liu, Xutian Xue, and Nian-Zhong Chen. 2021. "Fracture Mechanics-Based Mooring System Fatigue Analysis for a Spar-Based Floating Offshore Wind Turbine." Ocean Engineering 223

- (March):108618. https://doi.org/10.1016/j.oceaneng.2021.108618.
- GWEC, Global Offshore Wind Report 2023, 2023.
- Hall, Matthew, and Andrew Goupee. 2015. "Validation of a Lumped-Mass Mooring Line Model with DeepCwind Semisubmersible Model Test Data." *Ocean Engineering* 104 (August):590–603. https://doi.org/10.1016/j.oceaneng.2015.05.035.
- Lehmann, Marcus, Farid Karimpour, Clifford A. Goudey, Paul T.

  Jacobson, and Mohammad-Reza Alam. 2017. "Ocean
  Wave Energy in the United States: Current Status and
  Future Perspectives." *Renewable and Sustainable Energy Reviews* 74 (July):1300–1313.
  https://doi.org/10.1016/j.rser.2016.11.101.
- Ma, Kai-tung, Hongbo Shu, Philip Smedley, Didier L'Hostis, and Arun Duggal. 2013. "A Historical Review on Integrity Issues of Permanent Mooring Systems." *Offshore Technology Conference*, Houston, Texas, USA. https://doi.org/10.4043/24025-MS.
- Neary, Vincent S, Mirko Previsic, Richard A Jepsen, Michael J Lawson, Yi-Hsiang Yu, Andrea E Copping, Arnold A Fontaine, Kathleen C Hallett, and Dianne K Murray. 2014. "Methodology for Design and Economic Analysis of Marine Energy Conversion (MEC) Technologies."
- Ogden, David, Kelley Ruehl, Yi-Hsiang Yu, Adam Keester, Dominic Forbush, Jorge Leon, and Nathan Tom. 2022. "Review of WEC-Sim Development and Applications." *International Marine Energy Journal* 5 (3): 293–303. https://doi.org/10.36688/imej.5.293-303.
- Sørum, Stian H., Nuno Fonseca, Michael Kent, and Rui Pedro Faria. 2023. "Assessment of Nylon versus Polyester Ropes for Mooring of Floating Wind Turbines." *Ocean Engineering* 278 (June):114339. https://doi.org/10.1016/j.oceaneng.2023.114339.
- "Waves4Power." 2016 Waves 4 Power. Accessed July 8, 2024. https://www.waves4power.com/.
- "WEC-Sim Documentation." 2023. Accessed July 7, 2024. https://wec-sim.github.io/WEC-Sim/dev/user/applications.html#mooring.
- Wu, Yongyan, Tao Wang, Øyvind Eide, and Kevin Haverty. 2015. "Governing Factors and Locations of Fatigue Damage on Mooring Lines of Floating Structures." *Ocean Engineering* 96 (March):109–24. https://doi.org/10.1016/j.oceaneng.2014.12.036.
- Wu, Yongyan, Tao Wang, and Rolf Eide. 2015. "Governing Locations of Offshore Fatigue Design." *Proceedings of the 20<sup>th</sup> Offshore Symposium*, Houston, Texas.
- Xu, Sheng, Shan Wang, and C. Guedes Soares. 2019. "Review of Mooring Design for Floating Wave Energy Converters." *Renewable and Sustainable Energy Reviews* 111 (September):595–621. https://doi.org/10.1016/j.rser.2019.05.027.
- Xue, Xutian, Nian-Zhong Chen, Yongyan Wu, Yeping Xiong, and Yunhua Guo. 2018. "Mooring System Fatigue Analysis for a Semi-Submersible." *Ocean Engineering* 156 (May):550–63. https://doi.org/10.1016/j.oceaneng.2018.03.022.

- Yang, Shun-Han, Jonas W. Ringsberg, Erland Johnson, ZhiQiang Hu, and Johannes Palm. 2016. "A Comparison of Coupled and De-Coupled Simulation Procedures for the Fatigue Analysis of Wave Energy Converter Mooring Lines." *Ocean Engineering* 117 (May):332–45. https://doi.org/10.1016/j.oceaneng.2016.03.018.
- Yu, Y. H., D. S. Jenne, R. Thresher, A. Copping, S. Geerlofs, and L. A. Hanna. 2015. "Reference Model 5 (RM5): Oscillating Surge Wave Energy Converter." NREL/TP--5000-62861, 1169778. https://doi.org/10.2172/1169778.